Progress of Theoretical Physics, Vol. 56, No. 6, December 1976

Study of Multiple Meson Production at Cosmic Ray Energy. I

——Longitudinal Behaviour of Gamma Ray Air Family——

Eiichi KONISHI, Toru SHIBATA,* Edison H. SHIBUYA**
and Nobuhito TATEYAMA***

Science and Engineering Research Laboratory, Waseda University, Tokyo 160
**Department of Physics, Aoyama Gakuin University, Tokyo 158*
***Departamento de Fisica, Universidade de Campinas, Sao Paulo, Brasil*
****Faculty of Engineering, Kanagawa University, Yokohama 221*

(Received May 4, 1976)

Study of multiple meson production at cosmic ray energy, $10^{13}\sim10^{16}$ eV, based on the observation by emulsion chamber is performed. It is found that the effective multiplicity of gamma rays produced by nuclear interaction increases considerably as interaction energy gets higher, and is represented as $\propto(\sum E_\gamma)^{0.2\sim0.3}$. This result is consistent with the one obtained by the analysis of clean jets and also local nuclear interactions occurred in solid producing layers. Shower age analysis of gamma ray air family supports the increasing effective multiplicity of gamma rays. These are in reasonable agreement with the picture of two kinds of fireballs belonging to different levels—H- and SH-quanta.

§ 1. Introduction

During the time from May 1968 to April 1969, a huge thin type emulsion chamber (called CH. 14) was exposed on Mt. Chacaltaya by Japan-Brasil Emulsion Chamber Collaboration.[1] The area of CH. 14 (46.8 m^2) nearly equals total integrated one of previous chambers, CH. 1 to CH. 13. CH. 14 gave us various information on morphological studies, which had never been induced from previous small size chambers. After the exposure of CH. 14, a different type of chamber named CH. 15 was exposed for 300 days from September 1969.[1] CH. 15 was designed with an aim to observe local nuclear interactions occurred in an artificial producing layer. Interaction energy region of nuclear-active components observed by CH. 15 covers $10\sim100$ TeV. Some parts of morphological results of CH. 14 and CH. 15 were reported in the 13th International Cosmic Ray Conference.[2] Their essential points may be summarized as follows:

A) Integral energy spectra of electromagnetic and nuclear-active components are expressed by a simple power law with exponents 2.05 ± 0.05 and 1.80 ± 0.10, respectively up to $\sim10^{14}$ eV with many degrees of confidence.

B) Integral energy flow spectrum of gamma ray air family, $I(\geq\sum E_\gamma)$, is approximately given by a simple power function, $(\sum E_\gamma)^{-\beta}$, with $\beta=1.25\pm0.10$

from $\sim 10^{13}$ eV to $\sim 10^{15}$ eV.

C) Integral multiplicity spectrum of gamma ray air family, $I(\geq N_\gamma)$, is also expressed by a simple power function, $N_\gamma^{-\beta}$, with $\beta = 1.40 \pm 0.12$ for $N_\gamma \geq 4$.

D) Attenuation lengths for the intensity of electromagnetic components and energy flow of gamma ray air family are nearly the same and given as $\lambda_a = 90 \sim 100$ gr/cm^2, the results being directly obtained by a comparison with data observed on Mt. Norikura.

Morphological analysis of cosmic ray components observed by emulsion chamber has already been performed by many authors,[3] concentrating their attention on internal relations among various cosmic ray particles $(\gamma, e^{\pm}, N, \pi^{\pm}, \mu^{\pm}, \cdots)$ in the atmosphere. The energy region of those studies was restricted in at most $\sim 10^{13}$ eV, because of poor statistics at that time. On the other hand, CH. 14 and CH. 15 enable us to study electromagnetic and nuclear-active components with higher energy, 10$\sim$100 TeV. Moreover, if one treats the extensive gamma ray air family in the light of energy flow, then the energy region for morphological study extends up to $\sim 10^{15}$ eV. This energy may correspond to $\sim 10^{16}$ eV or more for primary nucleon. This point is the main motivation for the present paper.

The characteristic feature of constant mass fireball model is the validity of a similarity law for longitudinal motion of secondary particles; namely distribution function for the energy spectrum of secondary particles is expressed by a functional form, $f(E/E_0)dE/E_0$. Recently, also from accelerator experiment, this similarity law—scaling—was confirmed. Generally, as is easily expected, if the energy spectrum of secondary particles per interaction is given by a fractional form $f(E/E_0) \times dE/E_0$, then the exponent of electromagnetic energy flux is completely the same as that of nuclear-active flux. So the result A) suggests that mechanism of multiple meson production may change gradually as the interaction energy gets higher. In fact, Ref. 1) and recent analysis of CH. 15 by Japan-Brasil Collaboration[5] point out directly a possibility of existence of a super-heavy fire ball, abbreviated as SH-quantum.

From these standpoints in this paper, we shall study results A)$\sim$D), in connection with the possibility of broken similarity law.

§ 2. Mechanism of multiple meson production and basic assumptions

Throughout this paper, we neglect contribution of charged pions and kaons, generated by successive nuclear interactions, because of high detection threshold energy for atmospheric gamma rays in the case of emulsion chamber experiment.

a) *Primary nucleon spectrum*

In the morphological studies induced by CH. 14, interaction energy region remains at $10^{13} \sim 10^{15}$ eV. This energy region observed on Mt. Chacaltaya, may nearly correspond to $10^{14} \sim 10^{16}$ eV for primary nucleon spectrum, with consideration of the effect of inelasticity, collision mean free path and electromagnetic cascade

process in the atmosphere. Noticing recent data obtained by emulsion chamber[2),7)] (mainly from the spectrum of nuclear-active particles) and extensive air shower experiments[8)] (remarking the region around bending point), it seems appropriate to assume that integral primary nucleon spectrum concerned is approximately given as

$$F(\geq E_0) = I_0 E_0^{-\gamma}, \text{ with } \gamma = 1.8. \tag{2·1}$$

As for the absolute flux value I_0, it is found that there exists slight discrepancy[9),10)] between emulsion chamber and air shower results. So in the present paper, we shall study only relative values among various cosmic ray components, in order to avoid systematic under- or over-estimations for primary nucleon energy.

b) *Inelasticity distribution*

For a long time, it has been established through the cosmic ray observations[10)] that the inelasticity is on average ~ 0.5 and has a broad distribution. In this paper, we do not specify a definite distribution function, but give only the following general functional form:

$$\eta(K)\,dK, \text{ with } \int_0^1 \eta(K)\,dK = 1. \tag{2·2}$$

In the emulsion chamber experiment, one observes electromagnetic showers caused through $\pi^0 \to 2\gamma$ decay and the subsequent cascade process. So, behaviour of fraction of energies released into gamma ray components, k_γ, is often a critical problem for studying gamma ray air family and also local nuclear interactions occurred in the emulsion chamber. Of cource, k_γ-distribution is connected closely with K-distribution through charge fluctuation, but here we assume its functional form to have the following independent form:

$$\xi(k_\gamma)\,dk_\gamma, \quad \text{with} \quad \int_0^1 \xi(k_\gamma)\,dk_\gamma = 1. \tag{2·3}$$

c) *Production mechanism of secondary gamma rays*

In 1967, Japan-Brasil Emulsion Collaboration showed the existence of a constant mass fireball with constant temperature—H-quantum[4)]—as an intermediate product in super-high energy phenomena of multiple meson productions.[6)] As is given in Ref. 1), the energy and angular distribution of secondary gamma rays in the fireball rest system is given as

$$\psi(p^*, \theta^*)\,dp^*\,d(\cos\theta^*) = N_\gamma e^{-p^*/p_0} \frac{p^*\,dp^*}{2p_0^2}\,d(\cos\theta^*). \tag{2·4}$$

Here, N_γ is multiplicity of gamma rays produced by the decay of fireball and p_0 corresponds to average momentum of those in the fireball rest system, which are given in the energy region $10^{11} \sim 10^{13}$ eV as

$$N_\gamma = 8 \pm 1 \text{ and } p_0 = 82 \pm 15 \text{ MeV}/c, \tag{2·5}$$

respectively.

From Eq. (2·4) and the following well-known relations

$$p^* = \Gamma(E_\gamma - \beta E_\gamma \cos\theta) \simeq E_\gamma(1+\Gamma^2\theta^2)/2\Gamma\,, \tag{2·6a}$$

$$\sum E_\gamma \simeq M_\gamma \Gamma = 2N_\gamma p_0 \Gamma\,, \tag{2·6b}$$

where M_γ and Γ are the mass and the Lorentz factor, respectively, of the fireball converted into gamma rays, we get the energy and angular distribution in the laboratory system as

$$\left.\begin{aligned} f(E_\gamma, \boldsymbol{\theta})\, dE_\gamma d\boldsymbol{\theta}/\pi &= N_\gamma \exp\{-X(1+Y^2)\}\, dX\, dY^2 \\ \text{with} \qquad X &= N_\gamma E_\gamma / \sum E_\gamma \quad \text{and} \quad Y = \Gamma\theta\,. \end{aligned}\right\} \tag{2·7}$$

Integrations with respect to X and Y in Eq. (2·7) give

$$N_\gamma dY^2/(1+Y^2)^2\text{: isotropical angular distribution}\,, \tag{2·8a}$$

$$N_\gamma \exp(-X)\, dX\text{: exponential energy distribution}\,, \tag{2·8b}$$

respectively. Remembering that interaction energy $\sum E_\gamma$, in the laboratory system, is almost transferred into the fastest moving fireball, we can regard N_γ as an effective multiplicity of secondary gamma rays for the concerned nuclear interaction.

According to Refs. 1) and 6), it is indicated that there exists a possibility of giant fireball productions—SH-quantum—with $N_\gamma = 20 \sim 30$, particularly in the higher interaction energy region $\gtrsim 10^{14}$ eV. Therefore, in the present paper, we make the following trial assumption of increasing effective multiplicity with interaction energy:

$$N_\gamma = N_0 (\sum E_\gamma / 10^{12} eV)^\alpha\,, \tag{2·9}$$

giving superposed gross behaviour of two types of fireball productions.

§ 3. Formulation for the propagation of cosmic rays in the atmosphere

3. 1. *Nucleon component*

Nucleon energy spectrum

Let us consider the case that a nucleon with energy E_0 enters into the top of atmosphere. Then the energy spectrum of nucleon at depth t is immediately written down as

$$n_N(E_0, E_N, t)\, dE_N = \sum_{n=0}^{\infty} p_n(t/\lambda_c) f_n(E_0, E_N)\, dE_N\,, \tag{3·1}$$

where, λ_c is a collision mean free path of nucleon and $p_n(t/\lambda_c)$ represents poisson distribution. $f_n(E_0, E_N)$ is the energy distribution function after the incident primary nucleon has collided n-times with air nucleus. Combining the inelasticity distribution function $\eta(K_i)\, dK_i$ and the relation $K_i = 1 - E_i/E_{i-1}$, then $f_n(E_0, E_N)$ is represented as

$$f_n(E_0, E_N)\,dE_N = \int_{E_i \leq E_{i-1}} \cdots \int \eta(1-E_1/E_0)\,dE_1/E_0 \cdots \eta(1-E_N/E_{n-1})\,dE_N/E_{n-1}$$
$$= \frac{dE_N}{E_N}\frac{1}{2\pi i}\int_c ds \left(\frac{E_0}{E_N}\right)^s \left(\int_0^1 (1-x)^s \eta(x)\,dx\right)^n, \qquad (3\cdot 2)$$

where integral path c is running in the convergence domain parallel to the imaginary axis. Substituting Eq. (3·2) into Eq. (3·1) and summing up with respect to n, one can obtain

$$n_N(E_0, E_N, t)\,dE_N = \frac{dE_N}{E_N}\frac{1}{2\pi i}\int ds \left(\frac{E_0}{E_N}\right)^s e^{-t/\lambda_a(s)}, \qquad (3\cdot 3a)$$

$$\frac{1}{\lambda_a(s)} = \frac{1-\langle(1-K)^s\rangle}{\lambda_c}, \quad \text{with} \quad \langle(1-K)^s\rangle = \int_0^1 (1-x)^s \eta(x)\,dx\,. \qquad (3\cdot 3b)$$

Nuclear-active components

Nuclear-active components observed in emulsion chamber are almost dominated by nucleon, as far as the average inelasticity is ~ 0.5 over all the interaction energy region, because of high threshold energy of detection. In the case of emulsion chamber experiment, nuclear-active components are detected as the cascade shower, called Pb-jet, originated in lead plates of the chambers. Then, considering the effect of the primary nucleon flux, $\gamma I_0 E_0^{-(\gamma+1)} dE_0$, we obtain the integral energy flux of nuclear-active components as

$$I_N(\geq \sum E_r, T) = \int\int\int\int \gamma I_0 dE_0 E_0^{-(\gamma+1)} n_N(E_0, E_N, T)\,\xi(k_r)dk_r\,\delta(\sum E_r - k_r E_N)\,d(\sum E_r)\,dE_N$$
$$= I_0 \langle k_r^{\gamma}\rangle (\sum E_r)^{-\gamma} e^{-T/\lambda_a(\gamma)}, \qquad (3\cdot 4)$$

with

$$\langle k_r^{\gamma}\rangle = \int_0^1 z^{\gamma}\xi(z)\,dz\,. \qquad (3\cdot 5)$$

3. 2. *Electromagnetic components*

In the emulsion chamber experiment, the detection threshold energy of gamma rays and electrons is ~ 1 TeV, so that the approximation A in the cascade theory is available for the calculations concerned. Let us summarize the cascade function for multiplicity and energy flow in the following equations:

$$N_r(E_r', E_r, t) = \frac{1}{2\pi i}\int \frac{du}{u}(E_r'/E_r)^u N_1(u)\,e^{\lambda_1(u)t}, \qquad (3\cdot 6a)$$

$$\frac{\sum E_r(E_r', E_r, t)}{E_r} = \frac{1}{2\pi i}\int \frac{du}{u-1}(E_r'/E_r)^u N_1(u)\,e^{\lambda_1(u)t}, \qquad (3\cdot 6b)$$

with

$$N_1(u) = H_2(u) + \sqrt{u}M(u), \qquad (3\cdot 6c)$$

where, $H_2(u)$ and $M(u)$ are familiar functions found in articles of cascade theory.

Flux of electromagnetic components

From Eqs. (2·8b) and (3·4), production spectrum of gamma rays at the depth $(t, t+dt)$ is given by

$$p(E_\gamma', t)\,dE_\gamma'\,dt/\lambda_e = \frac{dt}{\lambda_e}\int_{E_\gamma'}^{\infty} d(\sum E_\gamma)\,\frac{dI_N(\geq\sum E_\gamma, t)}{d(\sum E_\gamma)}\,N_\gamma^{\,2}e^{-N_\gamma E_\gamma'/\sum E_\gamma}\frac{dE_\gamma'}{\sum E_\gamma}$$

$$\simeq I_0\langle k_\gamma^{\,\gamma}\rangle E_\gamma'^{\,-\beta-1}e^{-t/\lambda_a(\gamma)}\frac{\gamma}{1-\alpha}N_0^{1-\beta}\Gamma(1+\beta)\,dE_\gamma'\frac{dt}{\lambda_e}, \qquad (3\cdot7)$$

with

$$\beta=(\gamma-\alpha)/(1-\alpha). \qquad (3\cdot8)$$

Multiplying Eq. (3·7) by Eq. (3·6a) and performing the integration with respect to E_γ', we get integral energy flux of electromagnetic components at the depth T as

$$I_\gamma(\geq E_\gamma, T)=\int_0^T\frac{dt}{\lambda_e}\int_{E_\gamma}^{\infty}dE_\gamma'\,p(E_\gamma', t)\,N_\gamma(E_\gamma', E_\gamma, T-t)$$

$$=\frac{\gamma I_0}{\beta(\gamma)}E_\gamma^{-\beta(\gamma)}\Omega_\gamma(\gamma, T), \qquad (3\cdot9)$$

where

$$\Omega_\gamma(\gamma, T)=\langle k_\gamma^{\,\gamma}\rangle\frac{N_0^{1-\beta(\gamma)}}{1-\alpha}N_1(\beta(\gamma))\,\Gamma(1+\beta(\gamma))\frac{1}{\lambda_e\Lambda(\gamma)}(e^{\Lambda(\gamma)T}-1)\,e^{-T/\lambda_a(\gamma)}, \qquad (3\cdot10)$$

with

$$\Lambda(\gamma)=\lambda_1(\beta(\gamma))+1/\lambda_a(\gamma). \qquad (3\cdot11)$$

It should be kept in mind in Eq. (3·9) that the exponent of electromagnetic energy spectrum β, is connected with that of nuclear-active spectrum γ, in the way shown in Eq. (3·8).

Flux of gamma ray air family

Replacing the term $dI_N/d(\sum E_\gamma)$ in Eq. (3·7) by n_N defined in Eq. (3·3a), and performing the same procedure as Eq. (3·9), we can obtain multiplicity and energy flow of gamma ray air family (called the size of family), with the help of simple pole $u=\beta(s)$, when we fix the energy of primary nucleon E_0 in the following:

$$N_\gamma(E_0, E_\gamma, T)=\frac{1}{2\pi i}\int_{C_N}\frac{ds}{\beta(s)}\frac{E_0^{\,s}}{E_\gamma^{\,\beta}(s)}\Omega_\gamma(s, T), \qquad (3\cdot12a)$$

$$\frac{\sum E_\gamma(E_0, E_\gamma, T)}{E_\gamma}=\frac{1}{2\pi i}\int_{C_E}\frac{ds}{\beta(s)-1}\frac{E_0^{\,s}}{E_\gamma^{\,\beta}(s)}\Omega_\gamma(s, T). \qquad (3\cdot12b)$$

Integral paths C_N and C_E must run in parallel with the imaginary axis with

conditions $\mathrm{Re}(s)>\alpha$ and $\mathrm{Re}(s)>1$, respectively. Remembering the fact that the depth of Mt. Chacaltaya is sufficiently large ($T=14.5$ radiation length), one can find the following simple pole in the integrand:

$$\Lambda(\bar{s})=1/\lambda_a(\bar{s})+\lambda_1(\beta(\bar{s}))=0\,. \tag{3·13}$$

Physical meaning of parameter $\bar{s}$, obtained by solving the above equation (3·13), may be interpreted as follows. Phenomenon of gamma ray air family is understood as the mixture of nuclear cascade (mainly nucleon successive interactions) and electromagnetic cascade processes. The first term $1/\lambda_a(\bar{s})$ appeared in Eq. (3·13), corresponds to the attenuation of primary nucleon, while the second term $\lambda_1(\beta(s))$ corresponds to the development of electromagnetic cascade showers, originated from the neutral pions created in nuclear interactions. Then one can expect an equilibrium state between the decrease of primary nucleon and the growth of gamma ray air family in deep observation level, and the solution of Eq. (3·13), $\bar{s}$, gives an equilibrium age of the surviving nucleon. These arguments lead to the following results:

$$N_\gamma(E_0,E_\gamma,T)=\frac{1}{\beta(\bar{s})}\frac{\Lambda(\bar{s})}{\Lambda'(\bar{s})}\Omega_\gamma(\bar{s})\frac{E_0^{\bar{s}}}{E_\gamma^{\beta}(\bar{s})}e^{-T/\lambda_a(\bar{s})}, \tag{3·14a}$$

$$\frac{\sum E_\gamma(E_0,E_\gamma,T)}{E_\gamma}=\frac{1}{\beta(\bar{s})-1}\frac{\Lambda(\bar{s})}{\Lambda'(\bar{s})}\Omega_\gamma(\bar{s})\frac{E_0^{\bar{s}}}{E_\gamma^{\beta}(\bar{s})}e^{-T/\lambda_a(\bar{s})}, \tag{3·14b}$$

where

$$\Omega_\gamma(s)=\langle k_\gamma^{\,s}\rangle\frac{N_0^{1-\beta(s)}}{1-\alpha}N_1(\beta(s))\Gamma(1+\beta(s))\frac{-1}{\lambda_c\Lambda(s)}\,. \tag{3·15}$$

Finally, taking account of the primary spectrum $I_0E_0^{-\gamma}$, integral spectra of multiplicity and energy flow for extensive gamma ray air families at deep observation level T are summarized as

$$I(\geq f_N)=I_0\left(\frac{\Omega_\gamma(s)}{\beta(s)}\frac{\Lambda(s)}{\Lambda'(s)}\right)^{\gamma/s}E_\gamma^{-\beta(s)\gamma/s}f_N^{-\gamma/s}e^{-\gamma T/s\lambda_a(s)}, \tag{3·16a}$$

$$I(\geq f_E)=I_0\left(\frac{\Omega_\gamma(s)}{\beta(s)-1}\frac{\Lambda(s)}{\Lambda'(s)}\right)^{\gamma/s}E_\gamma^{-\beta(s)\gamma/s}f_E^{-\gamma/s}e^{-\gamma T/s\lambda_a(s)}, \tag{3·16b}$$

where we put $s=\bar{s}$, and $f_N=N_\gamma(\geq E_\gamma)$ and $f_E=\sum E_\gamma(\geq E_\gamma)/E_\gamma$.

It should be paid attention to that the power and attenuation length for size spectrum of gamma ray air families are γ/s and $s\lambda_a(s)/\gamma$, respectively, in the region $f_N,\ f_E\gg 1$. Furthermore, the difference between multiplicity and energy flow spectra appears only in the factors $[1/\beta(s)]^{\gamma/s}$, $[1/\{\beta(s)-1\}]^{\gamma/s}$.

§ 4. Comparison with experimental results

In § 3, we showed flux of various cosmic ray components, evaluated on the ba-

sis of several assumptions summarized in § 2. In this section, let us compare these expected flux values with experimental results, obtained by Japan-Brasil Emulsion Chamber Collaboration.

4. 1. *Flux of electromagnetic and nuclear-active components*

Integral flux of electromagnetic and nuclear-active components on Mt. Chacaltaya are given as[2]

$$\phi_{e,\gamma}(\geq E) = \phi_{e,\gamma}(10^{13}\mathrm{eV}) \times (E/10^{13}\mathrm{eV})^{-\beta}, \tag{4·1}$$

$$\phi_{N.A}(\geq E) = \phi_{N.A}(10^{13}\mathrm{eV}) \times (E/10^{13}\mathrm{eV})^{-\gamma}, \tag{4·2}$$

where

$$\phi_{e,\gamma}(10^{13}\mathrm{eV}) = 2.25 \times 10^{-11}/\mathrm{cm}^2\ \mathrm{sec}\ \mathrm{str}, \tag{4·3a}$$

$$\phi_{N.A}(10^{13}\mathrm{eV}) = 5.00 \times 10^{-11}/\mathrm{cm}^2\ \mathrm{sec}\ \mathrm{str}, \tag{4·3b}$$

and $\beta = 2.05 \pm 0.05$ and $\gamma = 1.80 \pm 0.10$.

In order to eliminate troublesome effect from the absolute primary nucleon flux I_0, let us divide Eq. (3·4) by Eq. (3·9). Then we get the following ratio of nuclear-active particle flux to electromagnetic one:

$$R(\mathrm{N.A}/\gamma) \simeq -\lambda_c \Lambda(\gamma) \frac{\gamma-\alpha}{\gamma} \frac{N_0^{\beta-1}}{\Gamma(1+\beta)} (E/10^{12}\ \mathrm{eV})^{\alpha(\gamma-1)/(1-\alpha)}. \tag{4·4}$$

Figure 1 presents the flux of electromagnetic and nuclear-active components, using power function expression with $\beta = 2.05$. As is often pointed out before, one finds the difference between the exponents of two spectra. Remembering the relation $\beta = (\gamma-\alpha)/(1-\alpha)$, the experimental results $\gamma = 1.80 \pm 0.10$, $\beta = 2.05 \pm 0.05$ give

$$\alpha = 0.24 \pm 0.08. \tag{4·5}$$

It should be remarked that effective multiplicity of gamma rays per interaction increases like the famous 1/4-law with interaction energy. Putting numerical values $\gamma = 1.8$, $\beta = 2.05$, $\lambda_a = 95\ \mathrm{gr/cm}^2$ (to be discussed in the next part) and $T = 540\ \mathrm{gr/cm}^2$, into Eq. (4·4), one can directly compare the experimental value of the ratio with the expected ones, corresponding to several cases of N_0, as is shown in Fig. 1. Then the most probable value of N_0 lies around 10 as far as we approve Eq. (4·5).

4. 2. *Attenuation length of various cosmic ray components*

The attenuation length of cosmic ray components is connected closely with the collision mean free path λ_c and the inelasticity K, as is given in Eq. (3·3b).

Recent emulsion chamber experiments[1,2] give the attenuation length of electromagnetic and nuclear-active components with energy larger than $E_c = 3$ TeV, as

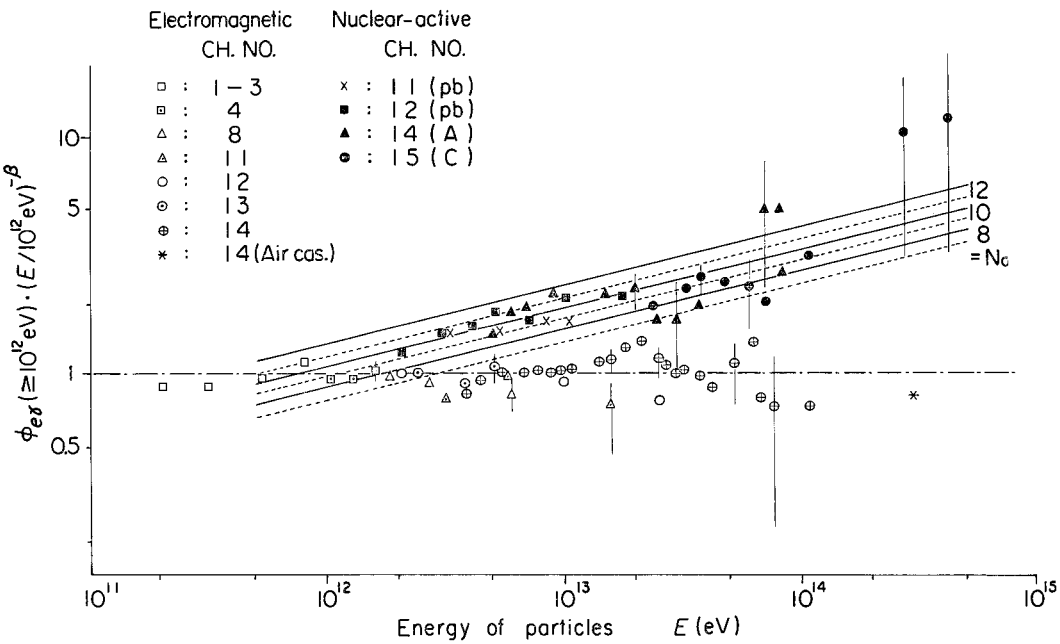

Fig. 1. Flux of electromagnetic and nuclear-active components expressed by power function form with $\beta=2.05$ and $\phi_{e,\gamma}(\geq 10^{12}\text{eV})=2.50\times 10^{-9}/\text{cm}^2\text{sec str}$. Solid and dotted lines correspond to the cases of constant (0.5) and uniform (0~1) inelasticity distributions, respectively.

$$\lambda_a=\begin{cases}95\pm 5\ \text{gr/cm}^2=2.50\pm 0.19\ \text{c.u.}, & (4\cdot 6a)\\ \text{for electromagnetic components,}\\ 100\pm 10\ \text{gr/cm}^2=2.63\pm 0.26\ \text{c.u.}, & (4\cdot 6b)\\ \text{for nuclear-active components.}\end{cases}$$

Now, let us consider two extreme cases of the inelasticity distribution with the mean value 0.5, that is to say, the one is the case of no fluctuation, the other is uniform one from 0 to 1. The real inelasticity distribution may be expected to lie between the above two. Putting $s=\gamma=1.8$ in Eq. (3·3b), one finds

$$\frac{\lambda_c}{\lambda_a}=1-\int_0^1(1-K)^{\gamma}\eta(K)\,dK$$

$$=\begin{cases}0.713 : \text{constant } \eta(K)=\delta(K-0.5), & (4\cdot 7a)\\ 0.643 : \text{uniform } \eta(K)=1. & (4\cdot 7b)\end{cases}$$

Comparing Eq. (4·6) with Eq. (4·7), one finds the collision mean free path is 60~70 gr/cm^2, which seems to be slightly smaller than the well-known one, 80 gr/cm^2, expected from geometric cross section of air nucleus.

The above result is for the single cosmic ray particles in the energy region

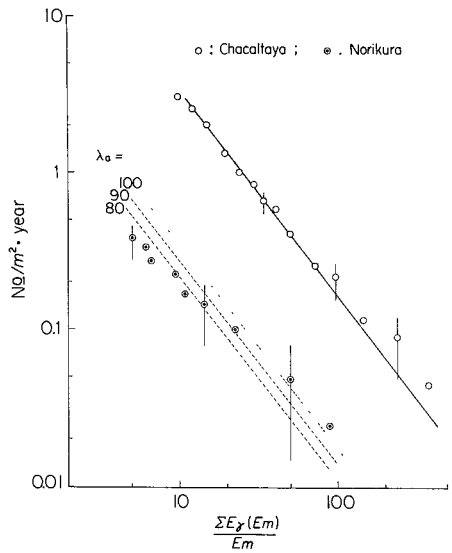

Fig. 2. Relative intensity of energy flow spectrum of air family observed on Mt. Norikura and Mt. Chacaltaya. Minimum detection energy of gamma rays is assumed as 2 TeV.

$\sim 10^{13}$ eV. However, making use of the energy flow intensity of gamma ray air families, one may be able to study the attenuation length of cosmic ray components in higher energy region (10$\sim$100 TeV). Let us show in Fig. 2 the relative intensity of energy flow of gamma ray air families observed on Mt. Norikura[12] and Mt. Chacaltaya. Drawing straight lines with exponent 1.3 (to be discussed in the next part), one finds

$$\Lambda_a = 90 \pm 30 \text{ gr/cm}^2 . \qquad (4\cdot 8)$$

On the other hand, study of zenith angle distribution for extensive air families obtained by CH. 14 gives

$$\Lambda_a = 110 \pm 25 \text{ gr/cm}^2 \qquad (4\cdot 9)$$

for the energy flow range $\sum E_\gamma \geq 50$ TeV.

As was shown in § 3, the attenuation length of gamma ray air families in the equilibrium state is given as

$$\Lambda_a = s\lambda_a(s)/\gamma . \qquad (4\cdot 10)$$

Here s is obtained by solving Eq. (3·13) of equilibrium state (to be discussed in the next part). Table I presents several cases of the attenuation length thus obtained. Unfortunately, however, it is difficult in this stage to get a definite conclusion about collision mean free path. We need more statistics of extensive air families in several observation points. So, in the present paper, we show only the general situation for the attenuation of gamma ray air families as mentioned above and leave the concluding discussion for future.

4. 3. *Multiplicity and energy flow of gamma ray air family*

Putting numerical values $\alpha = 0$, 0.2, 0.4 and $\lambda_c = 60$, 70, 80 gr/cm^2 in Eq.

Table I. Attenuation length corresponding to $\lambda_c = 60$, 70, 80 gr/cm^2, in the cases of two types of inelasticity distributions, constant and uniform ones.

	$\lambda_c = 60$ gr/cm^2		$\lambda_c = 70$ gr/cm^2		$\lambda_c = 80$ gr/cm^2	
α \ K	0.5	0$\sim$1	0.5	0$\sim$1	0.5	0$\sim$1
0	82.5	86.1	90.4	95.0	100	104
0.2	78.0	81.2	87.8	91.5	98.0	102
0.4	74.5	76.9	83.6	87.2	96.0	97.5

Table II. Shower age of air family in several cases.

α \ K	$\lambda_c=60$ gr/cm^2		$\lambda_c=70$ gr/cm^2		$\lambda_c=80$ gr/cm^2	
	0.5	0~1	0.5	0~1	0.5	0~1
0	1.72	1.58	1.50	1.44	1.40	1.36
0.2	1.51	1.44	1.37	1.34	1.30	1.28
0.4	1.31	1.31	1.25	1.24	1.21	1.20

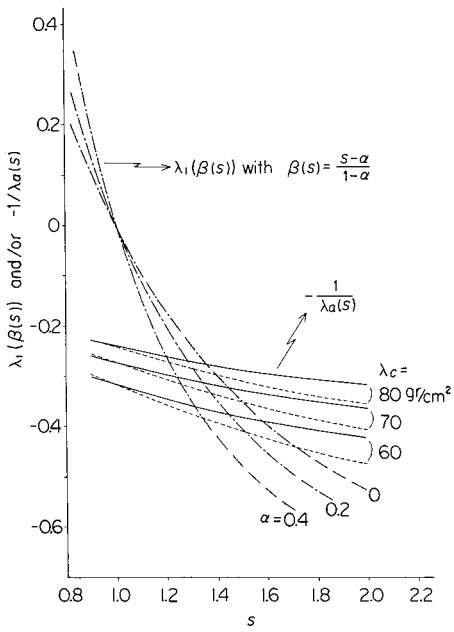

Fig. 3. Shower age of air family in the equilibrium state. Solid and dotted curves for $\lambda_a(s)$ correspond to the cases of constant (0.5) and uniform (0~1) inelasticity distributions, respectively.

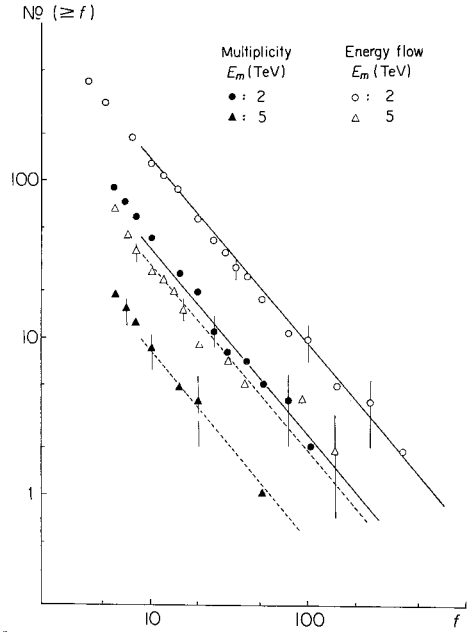

Fig. 4. Relative intensity between multiplicity and energy flux. f means $f_E=\sum E_\gamma(E_m)/E_m$ for energy flow and/or $f_N=N_\gamma(E_m)$ for multiplicity. All the straight lines are drawn with exponent 1.3.

(3·13), one can graphically evaluate the parameter s, as is drawn in Fig. 3. These results are summarized in Table II, corresponding to two typical cases of inelasticity distributions, constant and uniform ones, as is discussed in § 4.2.

Exponent of size spectrum for gamma ray air family

The exponents of multiplicity and energy flow spectra are obtained from CH. 14 as

$$\beta_N=1.40\pm0.12 \quad \text{for} \quad f_N=N_\gamma(\geq E_\gamma)\gtrsim 4\,, \tag{4·11a}$$

$$\beta_E=1.25\pm0.10 \quad \text{for} \quad f_E=\Sigma E_\gamma(\geq E_\gamma)/E_\gamma\gtrsim 10\,, \tag{4·11b}$$

respectively. Figure 4 shows the size spectrum—multiplicity and energy flow—in

the cases of $E_\gamma \geq 2$ and 5 TeV. In the last chapter, we showed that both exponents of multiplicity and energy flow spectra are equal to γ/s for the region f_N, $f_E \gtrsim 10$. Keeping our eyes upon the region f_N, $f_E \gtrsim 10$, we can draw a straight line with the following common exponent for the both spectra of multiplicity and energy flow:

$$\beta_N = \beta_E = 1.30 \pm 0.12 . \tag{4·12}$$

Equating the above value to γ/s, and putting $\gamma = 1.80$, one obtains the result

$$s = 1.38 \pm 0.13 . \tag{4·13}$$

Flux of air families

From Eqs. (3·16a) and (3·16b), we obtain the following flux ratio $R(N/E)$, between spectra of multiplicity and energy flow of gamma ray air families:

$$R(N/E) = \{(s-1)/(s-\alpha)\}^{\gamma/s} . \tag{4·14}$$

The experimental value of $R(N/E)$ is found from Fig. 4 as

$$R(N/E) = 0.26 \pm 0.04 . \tag{4·15}$$

Combining Eqs. (4·13), (4·14) and (4·15), and putting $\gamma = 1.8$, one gets

$$\alpha = 0.31 \pm 0.06 . \tag{4·16}$$

4. 4. *Comparison of flux values between electromagnetic components and gamma ray air family*

From Eqs. (3·9) and (3·16), we can estimate the expected relative intensity of air family to electromagnetic components. In those equations are included many parameters α, λ_c, k_γ, N_0. As for the parameter N_0, one gets the following dependence for the relative intensity from Eqs. (3·9) and (3·16):

$$R(F/\gamma) \propto N_0^{s(\gamma-s)/(1-\alpha)} . \tag{4·17}$$

Putting the typical numerical values $\gamma = 1.8$, $\alpha = 0.25$, $s = 1.4$, into Eq. (4·17), one finds the following dependence with respect to N_0:

$$R(F/\gamma) \propto N_0^{0.38} . \tag{4·18}$$

This is considerably weaker dependence than that of the case of the relative intensity between electromagnetic and nuclear-active components, which is expected from Eq. (4·4) (putting $\beta = 2.05$) as

$$R(\mathrm{N.A}/\gamma) \propto N_0^{1.05} . \tag{4·19}$$

Therefore, one finds that N_0 does not play so effective a part for the calculation of relative flux between electromagnetic components and gamma ray air families.

Remembering the last discussion, we put $\alpha = 0.25$ (or $\beta = 2.07$), $N_0 = 10$, $\lambda_c = 70$ gr/cm^2, and choose the following two extreme cases for k_γ-distribution, corresponding to two cases of K-distributions:

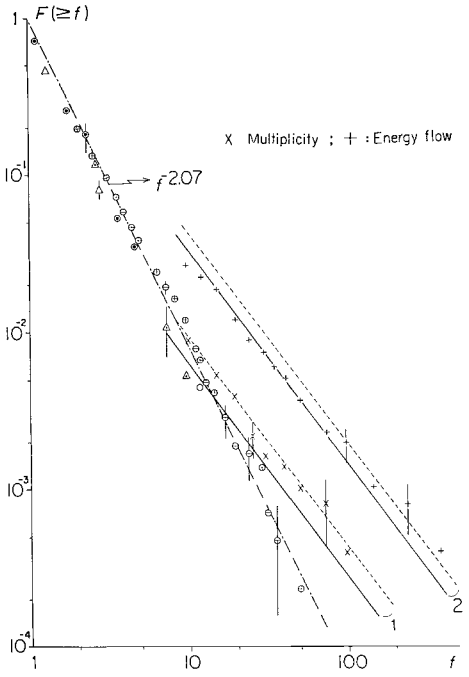

Fig. 5. Relative intensity between the sizes of air family and electromagnetic components.

$$f \equiv \begin{cases} E_\gamma/2\ \text{TeV} \\ \quad \text{for electromagnetic components,} \\ N_\gamma(\geq 2\ \text{TeV}) \\ \quad \text{for multiplicity of air family,} \\ \sum E_\gamma(\geq 2\ \text{TeV})/2\ \text{TeV} \\ \quad \text{for energy flow of air family.} \end{cases}$$

Groups 1 and 2 correspond to multiplicity and energy flow, respectively. Solid and dotted lines correspond to the cases of constant (0.5) and uniform (0~1) inelasticity distributions, respectively. $F(\geq f)$ is normalized by $\phi_{e,\gamma}(2\ \text{TeV}) = 6.80 \times 10^{-10}/\text{cm}^2\text{sec str}$. Marks of experimental plots for the spectrum of electromagnetic components are the same as in Fig. 1.

$$\hat{\xi}(k_\gamma)\,dk_\gamma = \begin{cases} \delta(k_\gamma - 0.167)\,dk_\gamma\,, & (4\cdot 20\text{a}) \\ 3.84\exp(-11.6k_\gamma^2)\,dk_\gamma\,. & (4\cdot 20\text{b}) \end{cases}$$

The mean value of k_γ is assumed as 1/6 in both the above equations, with the charge independence taken into account.

In Fig. 5, we present expected lines of relative flux between electromagnetic components and gamma ray air families, together with experimental points. It is remarkable that the sets of the numerical values $\alpha = 0.25$, $N_0 = 10$, estimated by the discussion in §§ 4.1 and 4.3, reproduce the observed relative intensity of air families to single electromagnetic components.

§ 5. Discussion and summary

The present paper is focused on the internal morphological relations among observed quantities of electromagnetic components, nuclear-active components and especially gamma ray air families. It became possible to draw a consistent picture for morphological behaviour of observed various cosmic ray components, as far as we limit the discussion within the emulsion chamber experiments. Before going to discussion of general problems related with other experimental evidences, let us summarize again several consequences presented in § 4.

N_0(effective multiplicity)

N_0 is discussed in §§ 4.1 and 4.4. As for the absolute value of N_0, we obtain

$N_0=10\pm2$, through the comparsion of flux ratio between electromagnetic and nuclear-active components. The value of N_0 thus obtained, reproduces well the expected intensity ratio between electromagnetic components and gamma ray air families.

The value $N_0=10\pm2$ is in agreement with the one $N_0=8\pm1$, obtained from the direct observation of local nuclear interactions.[1] However, we must recall that the latter includes a systematic bias for selected events, i.e., $N_r\geq4$, and after applying some corrections for such selection bias, N_0 is estimated as $4\sim6$[13] in the energy range $\sum E_r=10^{11}\sim10^{13}$ eV. Therefore, the present result $N_0=10\pm2$ indicates that SH-quanta are also generated with considerable frequency, together with H-quanta, in the interaction energy range $\sim10^{12}$ eV. This is expected from the direct evidences of SH-quantum production with gamma ray multiplicity $N_0=20\sim30$, as, for example, observed in the Chacaltaya CH. 15[5] data and the balloon data by Bristol-Bombay group.[11]

α (*multiplicity increase*)

All the experimental information presented in the last section, shows the increase of gamma ray multiplicity as $\propto E_0^{\alpha}$ with $\alpha\gtrsim0.2$.

First, in § 4.1, the difference between the exponents of electromagnetic and nuclear-active components spectra, leads to $\alpha=0.24\pm0.08$.

Secondly, in the analysis of the relation between multiplicity and energy flow of gamma ray air families, we are led to $\alpha=0.31\pm0.06$, in order to fit the consistent shower age for observed air families (discussed later).

Thirdly, it was checked that the intensity ratio between the electromagnetic components and air families is consistent with the assumption $\alpha=0.25$.

In the above three arguments, the latter two (study of air family) are more direct evidence for increasing effective multiplicity than the first one (study of single particle). This is because the slight systematic errors in the photometrical energy determination for single gamma ray and local nuclear interaction can give significant effect on the estimation by the first method. The calibration of photometrical method has been established by Ohta*[,14] in the energy region $\lesssim20$ TeV, but its extension to higher energy region was left for future. So, in the present stage, it would be safe to treat the spectra in the energy region $\lesssim20$ TeV with some reservation.

$\bar{s}$ (*shower age*)

From the exponent of air family spectrum observed on Mt. Chacaltaya, we found that $\bar{s}$ is equal to 1.38 ± 0.13. It is remarkable that the value $\bar{s}=1.38\pm0.13$ is reasonably expected from the equation of equilibrium state (3·13) under some choice of parameters K, α, λ_c, as is summarized in Table II. Here we should like to consider the meaning of $\bar{s}=1.38$. As was already mentioned in the end

*) Recently I. Ohta and his collaborators are trying to confirm the photometrical energy determination in higher energy region, with use of various types of X-ray films irradiated by electron beam of INS electron synchrotron.

of § 3, the parameter $\bar{s}$ does not mean the age of cascade shower in the usual sense, originated in single initial gamma ray, but the one of primary nucleon giving equilibrium state with gamma ray air family.

Corresponding to the case of single cascade shower age, we can regard $\lambda_1(\beta(s))$ $(=-1/\lambda_a(s))$ as the attenuation parameter of gamma ray air family. Then, an apparent shower age of gamma ray air family is given by $\beta(s)=(s-\alpha)/(1-\alpha)$. One finds immediately that as the parameter α(multiplicity increase of gamma rays), gets nearer to one, the apparent shower age of gamma ray air family becomes considerably old. So, one recognizes that the shower age study of gamma ray air family by means of the emulsion chamber, as well as the air shower experiment, is closely related to dynamics of multiple meson production through the magnitude of effective multiplicity. Recent analysis of energy spectrum of extensive gamma ray air family (200~700 TeV) observed at Mt. Fuji[15] gives a steep exponent with $\beta(s)\simeq 1.85$, the result of which suggests extreme high increase of multiplicity.

λ_c and K (collision mean free path and inelasticity)

Usually, in the observation concerning the cosmic ray propagation in the atmosphere, we cannot observe separately the collision mean free path λ_c and the inelasticity K, but their combination, as in the case of attenuation length.

Throughout the present paper, we assumed $\langle K\rangle=0.5$ when comparing the expected values of attenuation length with experiments, although we formulated the flux of cosmic ray components with a very general form of the inelasticity distribution $\eta(K)dK$. On the assumption $\langle K\rangle=0.5$, we find the collision mean free path λ_c is equal to 60~70 gr/cm^2, which value is estimated from the comparison of electromagnetic flux between Mt. Chacaltaya and Mt. Norikura. We have tried to study the collision mean free path λ_c also from the comparison of air family intensity between Mt. Chacaltaya and Mt. Norikura, and the zenith angle distribution of gamma ray air families. But, unfortunately, we could not get a definite conclusion for the collision mean free path λ_c in higher energy region at this stage, mainly because of limited observation range of energy at Mt. Norikura. Recently, however, big scale emulsion chamber experiments were started also at Mt. Fuji (630 gr/cm^2) by the Japanese group[9] and at Mt. Pamir (560 gr/cm^2) by the Soviet group.[16] Then, the above-mentioned ambiguities will be eliminated in the near future.

In the above concluding summary, there still remain the following further ambiguities.

The exponent of the primary nucleon flux in the energy range 10^{14}~10^{16} eV is assumed to be 1.8, as expected from the spectrum of the nuclear-active components observed on Mt. Chacaltaya and also from air shower experiments. The exponent of electromagnetic spectrum, 2.05 ± 0.05, is understood by introducing a parameter α with the value 0.24. It is well known that the exponent β_μ of μ-meson spectrum is related to that of gamma ray spectrum β as $\beta_\mu=\beta+1$. Then,

putting $\beta=2.05$, β_μ is expected to be 3.05. On the other hand, various recent direct observations of μ-meson spectrum[17] give $\beta_\mu=2.60\sim2.80$ in the energy region $10^{10}\sim10^{12}$ eV and the discrepancy between gamma ray and μ-meson spectra seems to be inevitable. However, when one observes cosmic ray components at a certain level, one must always remark the energy range of primary nucleon spectrum corresponding to that of detected cosmic ray components. As the main production height of μ-meson is considered to be very near to the top of atmosphere ($50\sim100$ gr/cm^2), the energy range of μ-meson spectrum, $10^{11}\sim10^{12}$ eV, corresponds to at most $10^{12}\sim10^{13}$ eV of primary nucleon spectrum, where the exponent is known as ~1.6. So, we may understand the discrepancy mentioned above not as derived from dynamical origin related with an elementary process, but as reflecting a "break" in the primary nucleon spectrum.

The last point to be mentioned is related to the mechanism of multiple meson production. We find that the effective multiplicity of gamma rays increases in the gross with interaction energy as

$$N_\gamma=(10\pm2)\times(\sum E_\gamma/10^{12}\text{ eV})^{0.2\sim0.3}. \tag{5·1}$$

Putting $\sum E_\gamma=10^{14}$ eV into Eq. (5·1), we get

$$N_\gamma=20\sim40. \tag{5·2}$$

The result is fairly consistent with that obtained directly from the analysis of clean jets[1] and also of the biggest event of local nuclear interaction ($\sum E_\gamma\sim80$ TeV) observed in CH. 15.[5]

The present paper is aimed at examining the gross behaviour of cosmic ray propagation on the basis of the fireball production with two different natures—H-quantum and SH-quantum—in super-high energy interactions. The consequence is that the morphological longitudinal behaviour of cosmic ray components, especially, extensive air families, is in reasonable agreement with the picture of the two kinds of the fireballs of different levels, H-quanta and SH-quanta.

As for the transverse behaviour of gamma ray air families, a preliminary analysis of CH. 14[18] reveals an extremely long tail of lateral distribution for superposed air families. This evidence may also be expected from SH-quantum which emits pions with larger transverse momentum than H-quantum. The study of transverse behaviour of air family will be reported in a subsequent paper.

Acknowledgements

We are very grateful to the members of Brazilian and Japanese emulsion chamber groups for offering us precious and enormous data of CH. 14 and CH. 15 with valuable discussion. In particular, we wish to thank Prof. C.M.G. Lattes, Prof. Y. Fujimoto and Prof. S. Hasegawa, who gave us guiding suggestions and valuable comments for the present paper. Thanks are also due to Prof. K. Yokoi

for his continuous encouragement with enlightening advice and careful reading of the manuscript.

References

1) a) Japanese and Brazilian Emulsion Chamber Groups, *Proceedings of the 11th International Conference on Cosmic Rays, Budapest 1969*, Vol. 3, HE 10.
   b) Japanese and Brazilian Emulsion Chamber Groups, Prog. Theor. Phys. Suppl. No. 47 (1971), 1.
   c) Japanese and Brazilian Emulsion Chamber Groups, *Conference papers, 12th International Conference on Cosmic Rays, Hobart 1971*, Vol. 7, pp. 2775, 2781, 2786.
2) Japanese and Brazilian Emulsion Chamber Groups, *Proceedings of the 13th International Cosmic Rays Conference, Denver 1973*, Vol. 3, p. 2219.
3) a) S. Hayakawa, J. Nishimura and Y. Yamamoto, Prog. Theor. Phys. Suppl. No. 32 (1964), 104.
   b) Japanese and Brazilian Emulsion Chamber Groups, *Proceedings of the International Conference on Cosmic Rays, London 1966*, Vol. 2, pp. 744, 835, 878.
   c) C. M. G. Lattes, Tese apresentada á Faculdade de Filosofia, Ciencia e Letras da Universidade de Sao Paulo para concurso á Catedra de Fisica Superior.
   d) A. Ohsawa, Prog. Theor. Phys. Suppl. No. 47 (1971), 180.
   e) K. Kasahara, Y. Fujimoto, S. Hasegawa, N. Ogita, A. Ohsawa and T. Shibata, Prog. Theor. Phys. Suppl. No. 47 (1971), 246.
   f) C. Santos, Dr. Thesis (Universidade de Estadual de Campinas, Sao Paulo, Brazil), 1972.
   4) S. Hasegawa, Prog. Theor. Phys. **26** (1961), 150; **29** (1963), 128.
5) Japanese and Brazilian Emulsion Chamber Groups, *Proceedings of the 13th International Cosmic Ray Conference, Denver 1973*, Vol. 3, p. 2210.
6) Japanese and Brazilian Emulsion Chamber Groups, Can. J. Phys. **47** (1968), 660.
7) T. Taira, T. Yuda, K. Taira, M. Shibata and K. Yokoi, *Proceedings of the 13th International Cosmic Ray Conference, Denver 1973*, Vol. 3, p. 2257.
8) a) J. Linsley, *Proceedings of the International Conference on Cosmic Rays, Jaipur 1963*, Vol. 4, p. 77.
   b) M. Lapointe, K. Kamata, J. Gaebler, I. Escobar, V. Domingo, K. Suga, K. Murakami, Y. Toyoda and S. Shibata, *Proceedings of the 10th International Conference on Cosmic Rays, Calgary* (1967), Part B, EAS 16 in press.
   c) S. I. Nikolsky, *Proceedings of the 15th Interamerican Seminar on Cosmic Rays*, II (1962), XLVIII.
   d) K. Greisen, Ann. Rev. Nucl. Sci. **10** (1960), 63.
   e) N. Grigorov, V. E. Nesterov and I. D. Rapoport, *Proceedings of the 10th International Conference on Cosmic Rays, Calgary 1967*, Part B, p. 512.
   f) V. V. Akimov, N. L. Grigorov, N. A. Mamontova, V. E. Nesterov, V. L. Prokhin, I. D. Rapoport and I. A. Savenko, *International Conference on Cosmic Rays, Budapest 1969*, Vol. 3, p. 211.
   g) G. Tanahashi, private communication.
9) I. Ohta, K. Kasahara, I. Mito, A. Ohsawa, T. Taira and S. Torii, *Proceedings of the 13th International Cosmic Ray Conference, Denver 1973*, Vol. 3, p. 2250.
10) a) P. H. Perkins, Progress in Elementary Particles and Cosmic Ray Physics **5** (1960), 259.
   b) L. F. Hansen and W. B. Fretter, Phys. Rev. **118** (1960), 812.
   c) V. V. Guseva, N. A. Dobrotin, N. G. Zelevinskaya and S. A. Slavatinsky, *Proceedings of the International Conference on Cosmic Rays and the Earth Storm, Kyoto 1961*, Vol. 3, p. 375.
   d) M. Koshiba, C. H. Tsao, C. L. Deney, R. Friken, R. W. Hugget, B. Hildebrand, R. Sillberberg and J. J. Lord, Nuovo Cim. Suppl. 1, No. 4 (1963a), 1091.

11) P. K. Malhotra, P. G. Shulka, S. A. Stephens, B. Vijayahshimi, J. Boult, M. G. Bowler, H. L. Hackforth, J. Keereetaveep, V. M. Mayes and S. N. Tovey, Nuovo Cim. **40A** (1965), 404.
12) M. Akashi, Z. Watanabe, N. Ogita, A. Misaki, I. Mito, Y. Oyama, S. Tokunaga, T. Ogata, Y. Tsuneoka, A. Nishio, S. Dake, K. Yokoi, S. Hasegawa, J. Nishimura, K. Niu, T. Taira and Y. Fujimoto, INS Report TCB-4, University of Tokyo (1965).
13) Y. Sato, T. Yanagida and N. Ogita, Prog. Theor. Phys. Suppl. No. 47 (1971), 214.
14) I. Ohta, Prog. Theor. Phys. Suppl. No. 47 (1971), 271.
15) I. Mito, K. Kasahara, A. Ohsawa, I. Ohta and S. Torii, Uchusen-Kenkyu (mimeographed circular in Japanese), Vol. 19, No. 3.
16) Y. V. Anischenko, L. T. Baradzei, N. A. Dobrotin, V. G. Dobrotin, V. G. Denisova, N. G. Zelevinskaya, E. A. Kanevskaya, V. M. Maximenko, V. S. Pushkov, S. A. Slavatinsky, Y. A. Smorodin, E. A. Solopov, G. T. Zatsepin, Z. A. Azimov, I. B. Bobodjanov, N. E. Scurchinskaya, N. G. Rjabova, G. B. Khristiansen, E. L. Andronikashvili, L. K. Chadranyan and L. A. Khizanishvili, *Proceedings of the International Cosmic Ray Conference, Denver 1973*, Vol. 3, p. 2228.
17) a) L. K. Ng, J. Wdowczyk and A. W. Wolfendale, *International Cosmic Ray Conference, Denver 1973*, Vol. 3, MN-2, p. 579.
b) R. P. Kokoulin, A. A. Pavlov, A. A. Petrukhin and V. V. Shestakov, *International Cosmic Ray Conference, Denver 1973*, Vol. 3, MN-2, p. 615.
c) M. S. Abdel-Monnem, J. R. Benbrook, A. R. Osborne, W. R. Sheldom, N. M. Duller and P. J. Green, *International Cosmic Ray Conference, Denver 1973*, Vol. 3, MN-2, p. 118.
d) Y. Takahashi, T. Shirai, K. Mizutani, A. Misaki, Z. Watanabe and M. Akashi, private communication.
18) E. Konishi and N. Tateyama, private communication.